Determination of wind energy from SAR images for siting windmill locations

O. M. Johannessen* & Erik Korsbakken

Nansen Environmental and Remote Sensing Centre
Edv.Griegsvei 3a, N-5037 Solheimsviken, Bergen, Norway
Phone: +47-55.297288, Fax: +47-55.200050, E-mail: Ola.Johannessen@nrsc.no
* Also at the Geophysical Institute, University of Bergen

Satellite-based Synthetic Aperture Radar (SAR) measurements from the European Space Agency (ESA) are proposed for wind-energy mapping in coastal regions for windmill location siting. The instrument has clear advantages for high-spatial resolution wind-field mapping since it is independent of daylight and clouds. The instrument's spatial resolution of 30 m is sufficient as is the 100 km-wide and several hundred km-long spatial coverage along the coastline. Wind maps generated from SAR will be able to provide spatial information concerning wind energy at 10m height in the vertical plane. We have, for the first time, used SAR for wind-energy mapping along a coastline and suggest that this can be an important method for selecting optimum locations for planned windmill parks.

Introduction

The Earth's population is facing an increasing demand for electrical power. After the recent Kyoto meeting, which gave clear signals of reductions in the CO_2 emission to the atmosphere, it is clear that new alternative sources of power must be considered to meet these needs. In this context, the possibilities for increasing the utilisation of converting wind energy into electrical power by use of windmills have been investigated. With the technical improvement of wind power turbines in recent years, operating wind power plants have become more economically efficient, and is today a worthy source for complementing other types of energy. For example, 7% of Danish power consumption, supplying about 200.000 households, are wind generated *[www.windpower.dk]*.

Energy of area exposed for wind vs. wind speed.

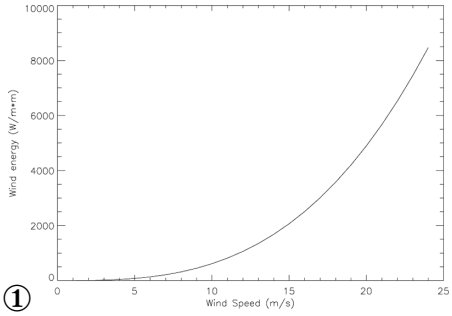

①

In planning for windmill park installations it is of fundamental importance to have sufficient information about the wind characteristics for different seasons. Standard wind measurements are available from ground mounted instruments, such as cup- or sonic anemometers, which usually provide a time series at an average of 1- or 10-minute intervals. Such measurements are localised and will not properly resolve the spatial variations in the wind field, and it is generally difficult to estimate wind conditions at a nearby site. From atmospheric boundary layer meteorology, we know that the surface wind field will have large spatial variations and the mapping of the wind field with high spatial resolution will be of great importance for the siting of windmill locations.

Figure 1 illustrates the importance of optimum location siting. The wind energy is proportional to the wind speed: $E = 0.5 \bullet 1.225 \bullet v^3$, where v is the wind speed in m/s, for air density of 1.225 kg/m^3, corresponding to dry air at standard atmospheric pressure at sea level at 15°C. With an average wind speed of 4.5 m/s at hub height (50-100 m), the average windmill will generate about 500 000 kWh per year. With an average wind speed of 9 m/s, it will generate 2 400 000 kWh per year. Therefore, doubling the average wind speed has increased energy output 4.8 times again, emphasising the importance of proper wind information for selecting optimum sites.

Left: SAR image from the west coast of Norway. Right: the corresponding wind energy map at 10 m height. Brighter areas indicates more wind energy as seen from the scale bar.

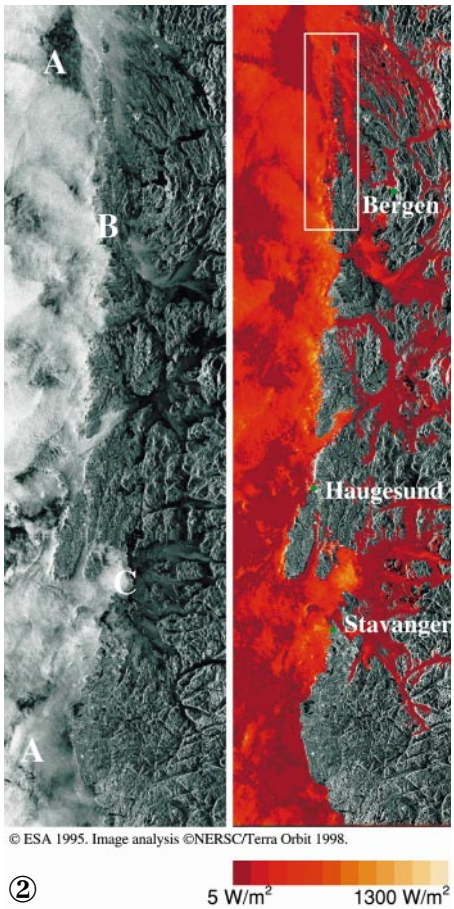

②

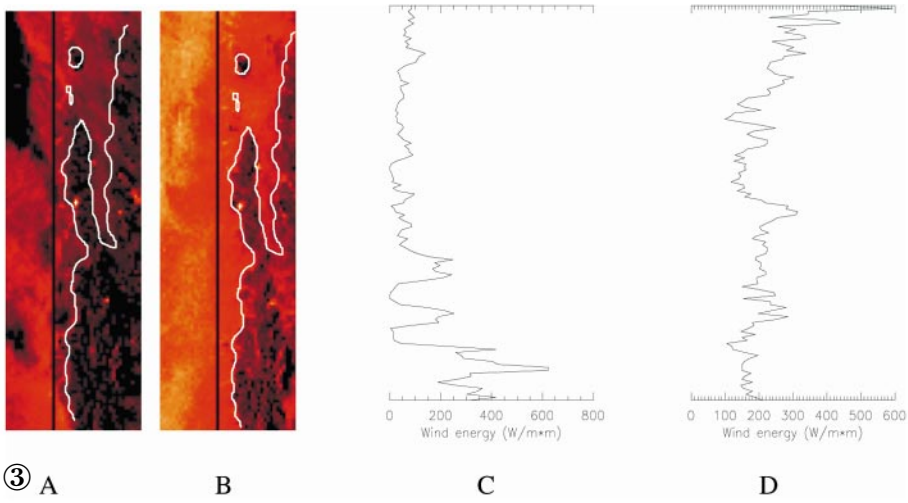

A) An extract corresponding to boxed area in Fig.2 from energy plot. B) energy plot from corresponding area from the SAR image taken the day before. The white line indicates a very rough land mask. C and D show the corresponding energy profile taken along the black lines line in A and B. Nearly twice as much energy will be available along the profile in the centre image due to higher average wind speed.

In our study of high spatial variations of wind energy along the coastline, we can now propose the use of high-resolution SAR wind measurements as complementary information. The SAR has clear advantages in being able to operate under all atmospheric conditions and independently of daylight and clouds. The SAR spatial resolution of ~30 m is sufficient for the application presented here. The major limitation is the relative poor temporal resolution and the demand for knowledge about wind direction as will be discussed later.

In the next section we will discuss the method of wind-energy retrieval from SAR data with examples. Finally, we will conclude and give future recommendations.

Data analysis

In the incidence angle range of ERS-1 and ERS-2 SAR (19°-26°) the reflected amount of energy will be proportional to a power of the surface wind speed. The radar signal is reflected in a system of short ocean capillary waves on a scale comparable to the wavelength (~5 cm) of the signal. This wave will be created instantly with the wind speed and is therefore an indicator of the surface wind speed. During several experiments, empirical relations between the wind speed (normalised to 10 m above the surface) and the received reflected radar signal from the surface are established. These relations are known as C-band models (CMOD) and their applications and accuracy for SAR is reported in e.g. *Vachon et al.* [1996], *Scoon et al.* [1996] and *Korsbakken et al.* [1997]. For wind-energy mapping, the spatial distribution of the wind speed, as derived using the CMOD Ifremer (Institut Français de Recherche pour l'Exploitation de la Mer) algorithm [*Quilfen et al.* 1997], is turned into wind energy using the above relation.

The CMOD Ifremer is calibrated against *in-situ* wind measurements, in particular the National Oceanic and Atmospheric Administration (NOAA) buoys (3433 collocated pairs) and the European Centre for Medium-Range Weather Forecasts (ECMWF) model results. The accuracy of such a model is better than –2 m/s for a single retrieval. The ESA SAR precision image format (SAR.PRI) is used because of its suitability for absolute calibration, which is necessary when using the above model. The SAR.PRI has an initial spatial resolution of about 30 · 30 m but to obtain satisfactory statistical significance the images are block averaged to a spatial resolution of 400 · 400 m, still allowing detailed mapping of the wind energy into the coastline.

The SAR-derived wind speed is normalised to 10 m height above the ocean surface using the CMOD Ifremer. Hub heights of modern 600 to 1500 kW wind turbines are usually 50 to 100 m. It is widely known that the wind speed increases rapidly with height in the surface boundary layer and that the wind estimates have to be corrected in order to be in the standard height of wind turbines. Note that the energy content of the wind varies with the third power of the wind speed so this correction becomes significant. In order to calculate the more accurate correction as a function height, we need to know the atmospheric stability, which is expressed as the difference of air and sea temperature.

Figure 2 shows an example of a SAR image and corresponding energy field of the average vertical energy at 10 m height for 400 · 400 m pixels projected down in the horizontal plane. The area is the west coast of Norway. In the SAR image we have indicated dark areas with low wind speed (A), bright areas with higher wind close to the shore (B),

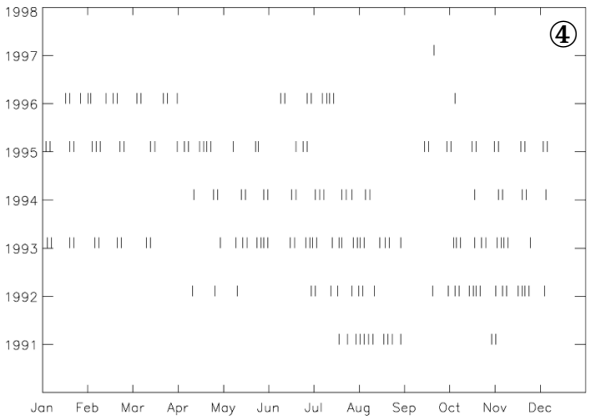

Temporal distribution of ERS-1 SAR data from 1991 covering the boxed area in Figure 2. From 1997 the same area is covered by ERS-2.

wind front in a fjord area (C). The wind speed in this case ranges from below 2 m/s and up to about 8 m/s. The wind speeds were calculated using the average wind direction from a synoptic meteorological map of the area. The energy plot clearly reveals areas of low and high energy into the coast and fjord areas. The energy ranges from about 5 W/m^2 up to about 700 W/m^2. The total length of the image is about 300 km. More detailed studies have to be performed on smaller areas for detailed siting of windmill locations as, for example, shown in Figure 3. From the energy field, a profile is extracted along the black line. Such a profile will represent the total instant energy distribution over the distance. The corresponding total available energy over a distance is obtained by integrating (integrating what ?) along this profile. This kind of plot, arranged chronologically for several images, as shown in Figure 3 for only two days, will clearly reveal low, frequent variations as seasonal dependence and regional persistency in energy distribution. Figure 4 illustrates the frequency of the available archived SAR data in the same region as shown above and the potential to further elucidate the area.

It is clear from the relative low temporal resolution of SAR images that repeated series of SAR images will not completely resolve temporal variations with scales of less than the SAR revisiting time. To get an optimal overview in both time and space, these 'time gaps' have to be filled with other information such as high-resolution meteorological models for flow studies, as well as *in-situ* measurements.

So far, we have shown that SAR images reveal intensity variations in the coastal zone and it is expected that these variations are caused only by wind-speed variations. However, sometimes the intensity is modulated by features such as natural- or man-made surface slicks [*Espedal et al.* 1998a, b], currents [*Johannessen et al.* 1998; *Jenkins et al.* 1997] or breaking waves. Still, if one or several of these effects are present, their influence on the wind speed will be weak when wind estimates are made by averaging over a larger area. The effect of breaking waves is often seen in a narrow belt (~100 m) very close to the coastline. This belt should, however, be excluded from the analysis because it will also contain pixels from land due to averaging. Effects of surface slicks may cause problems since the extension may be large and it can be difficult to distinguish them from real low-wind areas. The damping effect of natural slicks will disappear if the wind speed exceeds about 7 m/s [*Scott* 1985] and [*Espedal et al*. 1998]. Man-made slicks (e.g. oil leaking from ships) may be easier to distinguish in the SAR image because the extent is smaller and the damping is usually higher than for natural slicks. Future studies of repeated SAR data for an area will average out the majority of the errors discussed.

Conclusion

We have, for the first time, presented a method where SAR data are used to calculate high-resolution wind-energy maps as an addition to *in-situ* measurements for determining the location of windmill parks. The SAR-derived vertical-energy maps should be considered as complementary to standard meteorological field measurements and to model simulations. Once an area has been identified as promising from a SAR-based wind-energy atlas, local measurements, together with high-resolution models, must reveal the effect of local topography, etc. Standard measurements will also be of importance to partly compensate for the relatively poor temporal resolution of the SAR data. A comprehensive project including SAR data analysis, collection of *in-situ* data and wind modelling should be conducted to fully explore the optimal use of SAR for the siting of windmill locations.

Acknowledgements

The data for this demonstration was provided by the European Space Agency under the Announcement of Opportunity, AO2-N108. E. Korsbakken was supported by a SAR-strategy programme of the Nansen Centre, Norwegian Research Council.

References

Espedal HA, Oil spill and its look-alikes in ERS SAR imagery, Accepted in *Earth Obs. & Remote Sensing*, 1998 A.

Espedal HA et al.,Coastwatch '95: ERS-1/2 SAR detection of natural film on the ocean surface, Accepted in *JGR*, 1998 B.

Jenkins A et al., Intercomparison and improvement of SAR ocean imaging interaction models, NERSC Tech. Rep. no.132, Bergen, Norway, 1997.

Johannessen OM et al., Coastwatch: Using SAR imagery in an operational system for monitoring coastal currents, wind, surfactants and oil spills, in: *Operational Oceanography; The Challenge for European Co-operation*, eds. JH Stel, HWA Behrens, JC Borst, LJ Droppert & J vander Meulen, Elsevier Oceanography Series, The Netherlands. 1997

Johannessen OM et al., Coast Watch'95 ERS-1,2 SAR applications of mesoscale upper ocean and atmospheric boundary layer processes off the coast of Norway, *IGARSS'96*, Lincoln, NE, 1996.

Korsbakken E, JA Johannessen & OM Johannessen, Coastal wind field retrievals from ERS SAR images, accepted in *JGR*, 8 Sept. 1997.

Scoon A, IS Robinson & PJ Meadows, Demonstration of an improved calibration scheme for ERS-1 SAR imagery using a scatterometer wind model, *Int. J. Remote Sens*. **17** (2), 413-418, 1996.

Scott J , Surface films in oceanography, ONRL Workshop Report C-11-86, 1986.

Vachon PW & FW Dobson, Validation of wind vector retrieval from ERS-1 SAR images over the ocean, *The Global Atm. and Ocean Sys.* **5**, 177-187, 1996.

Quilfen Y, B Chapron, T Elfouhaily, K Katsaros & J Tournadre, Observation of tropical cyclones by high-resolution scatterometry, accepted in *JGR, 3* July 1997.